Combined Computational and Experimental Study the Effect of Doped Magnesium into Betanine-sensitized TiO_2 Photoanode for Dye-Sensitized Solar Cells Application

Yuly Kusumawati[1,*], Nanik Ismi Oktavianti[1], Linda Wati Oktavia[1], Nurul Widiastuti[1], Lukman Atmaja[1], Nur Izzati Abu Bakar[2], and Nur Hadi[2]

[1]*Department of Chemistry, Institut Teknologi Sepuluh Nopember, ITS Sukolilo campus, Surabaya 60111, East Java, Indonesia*

[2]*Ibnu Sina Institute for Fundamental Science Studies, University Teknologi Malaysia, Skudai, Malaysia*

* ***Corresponding author:***

email: y_kusumawati@chem.its.ac.id

Received: July 10, 2018
Accepted: December 22, 2018

DOI: 10.22146/ijc.36861

Abstract: *A preliminary study of the effect of magnesium-doped into betanine-sensitized TiO_2 thin layers has been carried out computationally and experimentally. The computational calculation was performed to observe the effect of magnesium on the interaction molecular of betanine onto TiO_2 surface, using $Ti_{12}O_{28}H_8$ model cluster. It was found out that the distance of the oxygen on the anchoring site betanine with the Ti in TiO_2/Mg cluster is shorter compare to that one in TiO_2 cluster. This result confirms the bond between betanine and TiO_2 is stronger in the case of Mg^{2+} incorporation. The Natural Population Calculation also confirms that the electron transport from betanine to the TiO_2 is more facilitated after Mg^{2+} incorporation. These results are also supported by the HOMO-LUMO profile of TiO_2-betanine and TiO_2/Mg. The XRD and SEM measurement confirm there are no effect on the TiO_2 structure and morphology with the incorporation of Mg^{2+}. The thin-film UV-Vis measurement confirms there is a bandgap shift after the incorporation of Mg.*

Keywords: *TiO_2; Mg-doped; betanine; DSSC*

■ INTRODUCTION

Development of device that converts solar energy to electricity has become the priority in the most countries in order to meet energy demand as the result of the abundant availability of solar energy for the next 40 years [1]. Moreover, solar energy is classified as clean renewable resources of energy. Dye-sensitized solar cells are one of the solar cell devices that are promising to be developed. Their fabrication is simple, moreover, they meet criteria as devices that are cost-effective and environmental friendliness. They consist of a mesoporous semiconductor layer deposited on a transparent conductive oxide (TCO), sensitized by a monolayer of dyes, and coupled with an electrolyte and a counter electrode. All components of DSSCs are desired to construct a stable and efficient solar cell device through their interactions at the molecular level. DSSCs can be small and light, so they can be easily applied to various electronic devices. They are mentioned as a candidate for the third generation of solar cells [2]. Despite their advantages, their efficiency is still lower compared to the silicone-based solar cells. The research to improve their performances has been on-going for more than two decades. This improvement covers the improvement of the semiconductor as photoelectrode, sensitizing dye, electrolytes or counter electrodes [3-6].

The purpose of DSSC development is not only to improve their performance but also to find the natural-source of DSSC components, in order to increase the economic value of some natural resources. One of the DSSC components that can be developed from the natural resources is dye sensitizer. Various researchers have found that a few natural dyes have a potential to be used as dye sensitizers such as anthocyanin, betanine/betalain, carotenoid, chlorophyll, and flavonoid [7-9]. The limitations of natural dyes in DSSC application are a lot of natural dyes do not have a good anchoring site [10] and the low stability of natural dyes

towards the photoelectrode [11]. Among the natural dyes, betanine is the most promising to be used as dye sensitizer due to owing the carboxylate functional group as good anchoring site to attach with TiO_2 surface [12] Whereas to increase dye stability towards the photoelectrode, Prabavaty et. al., have proposed various ways, one of the proposed ways is to create the electron trap site [11]. Metal-doped TiO_2 can become a method to create this trap. The various researches have been done to do metal-dopes TiO_2 [12-17]. Mg-doped TiO_2 has been studied and observed to apply for DSSC. The computational study has shown that there is a shift in bandgap after Mg-doped into TiO_2 [12-13]. Moreover, Liu has observed that the Mg-doped TiO_2 performance in DSSC application has higher short circuit current by 26.7% compared to undoped TiO_2 [17]. As far as we know, there has not been observed yet the study of the betanine utilization to sensitize Mg-doped TiO_2 for DSSC application. As well as the computationally study regarding the potency of Mg-doped TiO_2 for betanine-sensitize DSSC device.

In this work, we have investigated computationally and experimentally the effect of Mg-doped into betanine-sensitize TiO_2. In the case of TiO_2, the calculation was carried out using $Ti_{12}O_{28}H_8$ model cluster. The interaction of betanine with the TiO_2 and TiO_2/Mg surface has been observed. The natural population analysis (NPA) is calculated to find out the electron charge transfer from the betanine to the TiO_2. We also have figured out the HOMO and LUMO of the betanine -TiO_2 and betanine- TiO_2/Mg to reveal the effect of Mg into the electron transport from betanine to the photoelectrode.

■ EXPERIMENTAL SECTION

TiO_2 Particle Preparation

The synthesis of TiO_2 and TiO_2/Mg has been carried out using hydrothermal reaction based on reference [17]. 3 mL of acetic acid, 20 mL of butanol and 3 mL tetrabutyl titanate were mixed under constant mixing. 15 mL of butanol and 1 mL of water then was added to the mixture. The mixing process was continued for 30 min. The mixture then was moved into the hydrothermal reactor and put in the oven at 240 °C for 6 h. After cooled at room temperature, the mixture was centrifuged to get the deserved viscosity for thin-layer preparation using Doctor Blade technique. The Doctor Blade technique is a method for thin-layer preparation by depositing the slurry on the glass substrate using a thin glass. In this case, a microscope slide is commonly used to deposit the slurry. The same procedure was done for TiO_2/Mg. $Mg(NO_3)_2{\cdot}6H_2O$ was added into the mixture at 0.5; 1 and 1.5% mol of TiO_2. After the deposition process, the thin layer was annealed at 500 °C for 30 min [17].

Layer Characterization

The crystal structure was analyzed using X-ray Diffraction. The FTIR analysis was done using Shimadzu 8400S. The optical film properties (total transmission and total reflection) were recorded with a Carry 5000 UV-Vis-NIR spectrophotometer equipped with an integrating sphere which is located in Ibnu Sina Institut for Fundamental Science Studies, University Teknologi Malaysia, Skudai, Malaysia.

Computational Methods

The calculations were carried out using the Density Functional Theory (DFT) with the Gaussian 09 code [18] in custom-configured high-performance supercomputing, Ibnu Sina Institut for Fundamental Science Studies, University Teknologi Malaysia, Skudai, Malaysia. The optimization geometries were done using the B3LYP functional methods and 6-311G** [19]. Calculations were performed using B3LYP functionals. These methods have been chosen based on the consideration that B3LYP has been used widely in many calculations. B3LYP show the satisfactory results in calculating the ground states geometry even for such largely-conjugated molecules. The anatase (101) cluster, $Ti_{12}O_{28}H_8$ has been chosen as a representative model for TiO_2 layers. Slab anatase (101) was created using Avogadro software [20], the created slab then is cut and terminated by a Hydrogen atom. The input cluster of $Ti_{12}O_{28}H_8$ is shown in Fig. 1.

The optimized structure of TiO_2 cluster model then was analyzed it density of states (DOS) profile as shown in Fig. 2. Fig. 2 shows that this model has a conduction band value -3.8 eV and its valence band is -7.8 eV. These values are in agreement with the value of TiO_2 ones which are around -4 eV for conduction band

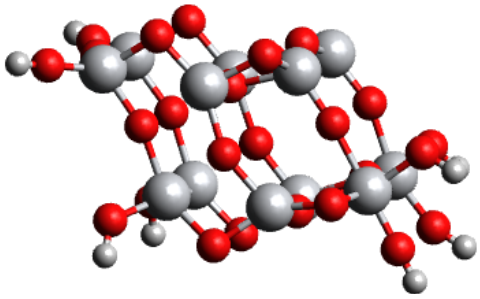

Fig 1. Anatase-$Ti_{12}O_{28}H_8$ cluster input model in this study, namely TiO_2. The small white ball = H; the big white ball = Ti; the red ball = Oxygen

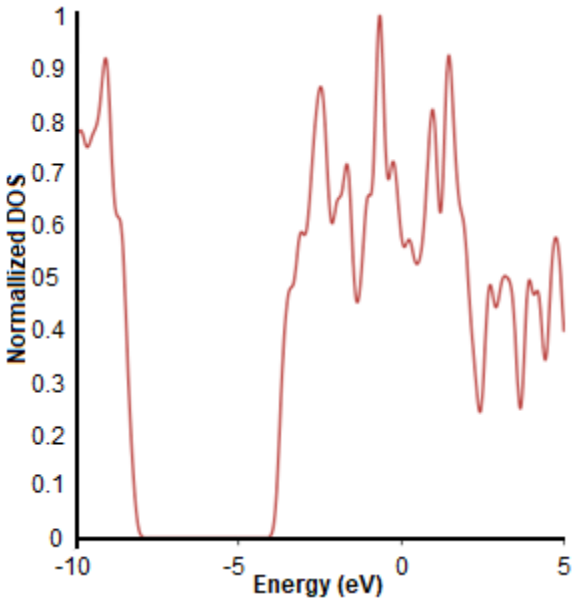

Fig 2. The DOS Plot of TiO_2 cluster model in this research

and -7.5 eV for the valence band [12-13]. Based on this result we continue using this model for the other calculations.

■ RESULTS AND DISCUSSION

The Effect of Mg into the TiO_2 Crystal-Structure

The effect of Mg^{2+} into the TiO_2 crystal structure is confirmed by the XRD analysis. The diffractogram of TiO_2/Mg compared to the pure TiO_2 is showed in Fig. 3. Fig. 3 confirms that the TiO_2 and TiO_2/Mg has an anatase structure (JCPDS card file no. 21-1272) that is confirmed by the peaks correspond to the Miller indices (101), (103), (004), (112), (200), (105), (211), (213), (204), (116), (220) and (215)).

On contrary, the result of optimization geometry of TiO_2 and TiO_2/Mg cluster show that the insertion of Mg^{2+} causes a small crystal distortion as displayed in Fig. 4. The change of the bond length of Ti and O around the

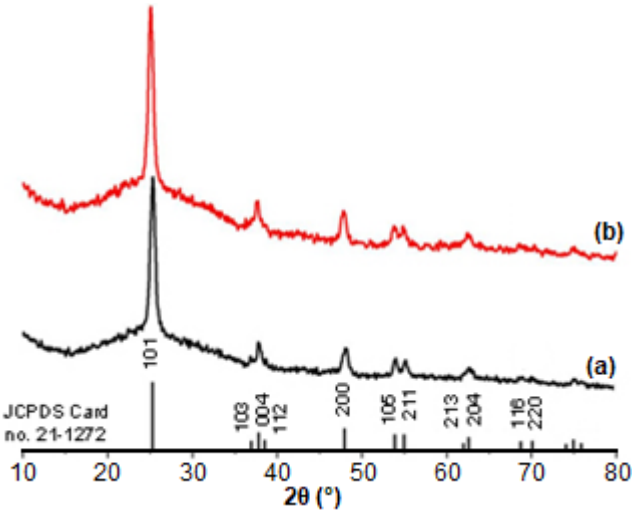

Fig 3. The diffractogram of (a) Pure TiO_2 and (b) TiO_2/Mg

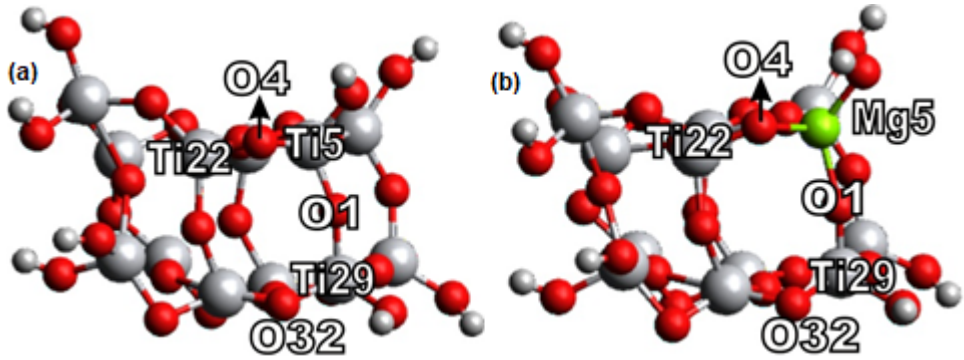

Fig 4. The optimization geometry result of (a) TiO_2 and (b) TiO_2/Mg cluster model. The small white ball = H; the big white ball = Ti; the red ball = Oxygen

Mg are listed in Table 1. Table 1 shows that the presence of Mg^{2+} will make the Oxygen atom move far away from the insertion position. This is due to the Mg^{2+} ionic radius (0.86 Å) is larger than Ti^{4+} one (0.74 Å) [13]. Moreover, the Ti^{4+} charge is larger than Mg^{2+} so the ionic interaction is stronger in the Ti-O system compare to the Mg-O system. Furthermore, this oxygen shift causes the atomic distance between O and the next Ti decrease. However, this small crystal distortion was not observed in the bulk system, probably because the Mg^{2+} concentration was too small. The same result was also observed in the diffractogram of TiO_2/Mg that was obtained by Gao et.al. They found that there was no significant difference in the diffractogram of TiO_2 and Mg-doped TiO_2 [15].

The Effect of Mg into the TiO_2 Electronic Properties

As predicted, the Mg-doped into TiO_2 provokes the bandgap shift. Fig. 5 shows the bandgap shift as a function of Mg concentration. The addition of 1.5% Mg makes the bandgap of TiO_2 decrease to 2.4 eV. This result is in agreement with the previous result showed by Kumar et. al. [22]. To find the explanation about the bandgap shift because of the Mg^{2+} incorporation, we then investigated the DOS profile of TiO_2 and TiO_2/Mg through the computational methods. The DOS profile of both systems is shown in Fig. 6.

Fig. 6 shows that there is a new localized state in the DOS profile of TiO_2/Mg that strongly suggest the occurrence of Ti-Mg interactions on the surface. These new localized states explain the bandgap shift for the system. The existence of new local states of Mg^{2+} was also observed by Liu et al. [16].

The Effect of Mg into the TiO_2 and Betanine Interaction

The betanine interaction with TiO_2 and TiO_2/Mg is confirmed in the FTIR measurement result that is shown in Fig. 7. The wide peak at the wave number range 2500–3500 cm^{-1} shows the O-H stretching vibration (1) and the wide peak at the wave number range 500–100 cm^{-1} shows the Ti-O-Ti stretch vibration (2) [23-25]. The peak at about 2900 cm^{-1} represents to C-H bond of betanine (3) [23]. The peak at about 1629 cm^{-1} is caused by O-H bending vibration [24]. A peak at 1029 cm^{-1}

Table 1. The list of bond length of Ti and O around the Mg

Bond length between	Bond length in TiO_2 cluster (Å)	Bond length in TiO_2/Mg cluster (Å)
Ti5-O1 or Mg5-O1	1.799	1.988
Ti5-O4 or Mg5-O4	1.899	2.012
Ti5-O1 or Mg5-O1	1.799	1.988
Ti22-O4	1.78	1.678
Ti27-O8	2.202	2.082
Ti29-O1	1.808	1.693
Ti29-O32	1.915	1.976

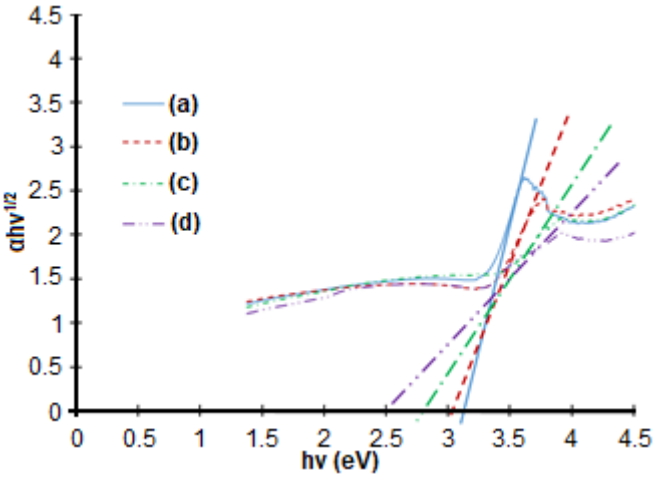

Fig 5. Bandgap calculation of (A) TiO_2; (B)TiO_2/Mg 0.5%; (C) TiO_2/Mg 1% and (D) TiO_2/Mg 1.5%

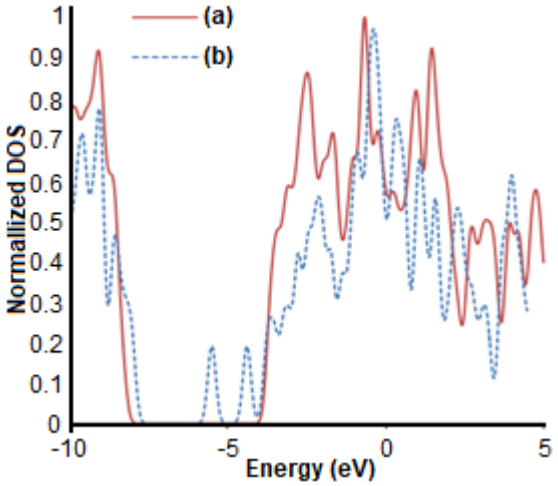

Fig 6. The DOS Plot of (A) TiO_2 cluster (B) TiO_2/Mg cluster

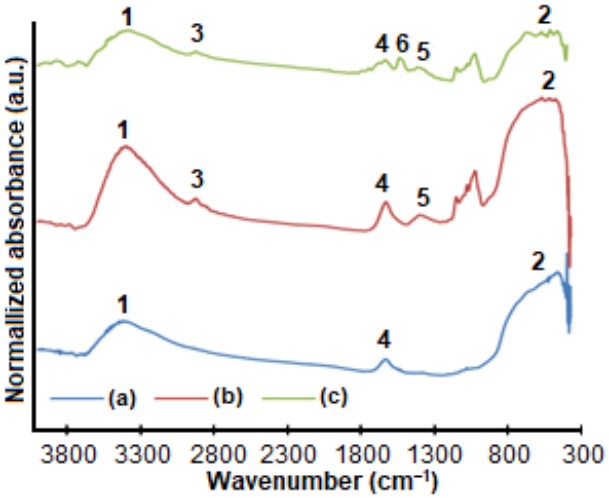

Fig 7. FTIR Spectrum of (a) TiO_2; (b) betanine-TiO_2 and (c) betanine-TiO_2/Mg

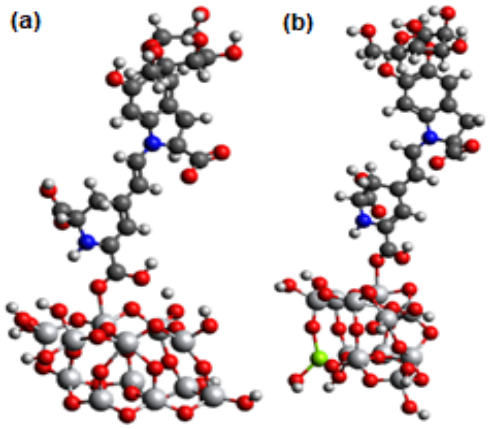

Fig 8. The results of optimization geometry betanine on TiO_2 and TiO_2/Mg surface. The small white ball = H; the big white ball = Ti; the red ball = Oxygen, the blue ball = N; the green ball = Mg

Table 2. Natural population analysis

	Natural Charge			
	Ti22	O4	O12	O21
In the betanine system	-	-	-	-
In the TiO_2 cluster	1.6975	-0.7600	-0.9064	-0.8413
In the TiO_2-cluster-betanine	1.6790	-0.7376	-0.8999	-0.8087
In the TiO_2/Mg cluster	1.6896	-0.8257	-0.9917	-0.8552
In the TiO_2/Mg cluster-betanine	1.6592	-0.8294	-0.9898	-0.8431

represents to C-O-C bond [25]. A peak at 1489 cm^{-1} represents Mg interaction with betanine (6) [26].

To figure out at the molecular level the effect of Mg^{2+} to theTiO_2 and betanine interaction, especially to the charge transfer properties, it is necessary to be performed using computational method since the experimental study is very limited.

The structure optimization of betanine on TiO_2 and TiO_2/Mg surface are shown in Fig. 8. In this figure, we can see that the distance of O atom in the anchoring site betanine with the Ti atom in the TiO_2 surface (2.20 Å) is shorter in the case of Mg incorporation (2.16 Å). This result indicates that betanine is attached stronger onto TiO_2/Mg surface than TiO_2. This condition will facilitate the electron transfer from betanine to the TiO_2. To make more clear about the electron transfer we have done the NPA analysis as shown in Table 2, completed with Fig. 9 to describe the corresponding atom in the Table. Table 2 shows that the Ti22 in TiO_2/Mg cluster receive more electron

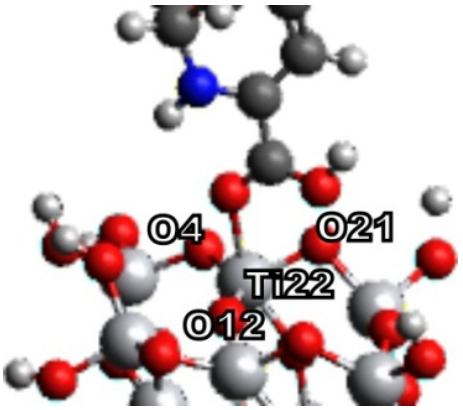

Fi 9. The corresponding atoms in the TiO_2 cluster, TiO_2/Mg cluster for Table 2. The small white ball = H; the big white ball = Ti; the red ball = Oxygen, the blue ball = N

compare to that one in TiO_2. This indicates that the electron is transferred more from betanine to the TiO_2/Mg compare to that one to the TiO_2. The profile of HOMO and LUMO of the betanine-TiO_2 and betanine-TiO_2/Mg support this suggestion. As presented in Fig. 10,

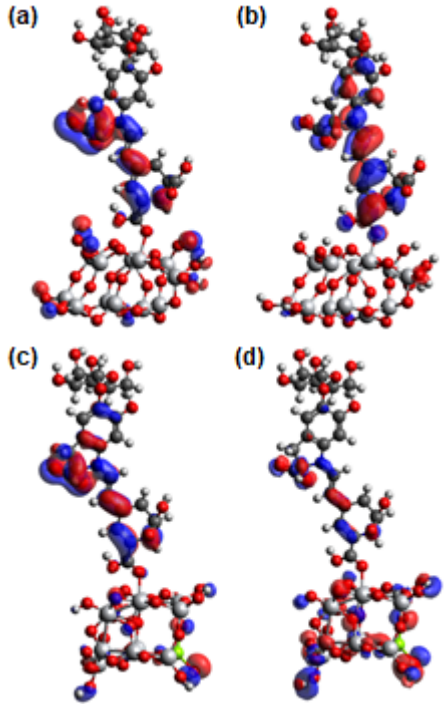

Fig 10. The profile of (a) HOMO betanine-TiO_2 (b) LUMO betanine-TiO_2 and (c) HOMO betanine-TiO_2/Mg and (d) LUMO betanine-TiO_2/Mg. The small white ball = H; the big white ball = Ti; the red ball = Oxygen, the blue ball = N; the green ball = Mg

the HOMO-LUMO calculation shows clearly that the electron preferable transfer into TiO_2 in the TiO_2/Mg system compares to the TiO_2 system.

■ CONCLUSION

The addition of 1.5% mole Mg^{2+} into TiO_2 is not changing the TiO_2 structure crystal even the calculation shows there is a small movement of oxygen position near to the insertion position. The bandgap of TiO_2 is being narrow with the increase of Mg^{2+} content in the TiO_2. The calculation result shows that Mg makes the interaction of betanine and TiO_2 stronger and support the electron transport from betanine to TiO_2. These results make TiO_2/Mg is promising to be sensitized by betanine to prepare photoanode for DSSCs application.

■ ACKNOWLEDGMENTS

The authors gratefully to the Institut Teknologi Sepuluh Nopember for funding this research through the Local Research Scheme.

■ REFERENCES

[1] Shafiee, S., and Topal, E., 2009, When will fossil fuel reserves be diminished?, *Energy Policy*, 37 (1), 181–189.

[2] Hagfeldt, A., Boschloo, G., Sun, L., Kloo, L., and Pettersson H, 2010, Dye-sensitized solar cells, *Chem. Rev.*, 110 (11), 6595–6663.

[3] Mathew, S., Yella, A., Gao, P., Humphry-Baker, R., Curchod, B.F.E., Ashari-Astani, N., Tavernelli, I., Rothlisberger, U., Nazeeruddin, M.K., and Grätzel, M., 2014, Dye-sensitized solar cells with 13% efficiency achieved through the molecular engineering of porphyrin sensitizers, *Nat. Chem.*,6 (3), 242–247.

[4] Shalini, S., Balasundaraprabhu, R., Kumar, T.S., Prabavathy, N., Senthilarasu, S., and Prasanna, S., 2016, Status and outlook of sensitized solar cells (DSSC): A review, *Int. J. Energy Res.*, 40 (10), 1303–1320.

[5] Ahmad, M.S., Pandey, A.K., and Rahim, N.A., 2017, Advancements in the development of TiO_2 photoanodes and its fabrication methods for dye-sensitized solar cells (DSSC) application. A review, *Renewable Sustainable Energy Rev.*, 77, 89–108.

[6] Kusumawati, Y., Martoprawiro, M.A., and Pauporté, T., 2014, Effects of graphene in graphene/TiO_2 composite films applied to solar cell photoelectrode, *J. Phys. Chem. C*, 118 (19), 9974–9981.

[7] Ludin, N.A., Mahmoud, A.M.A., Mohamad, A.B., Kadhum, A.A.H., Sopian, K., and Karim, N.S.A., 2014, Review on the development of natural dye photosensitizer for dye-sensitized solar cells, *Renewable Sustainable Energy Rev.*, 31, 386–396.

[8] Luo, P., Niu, H., Zheng, G., Bai, X., Zhang, M., and Wang, W., 2009, From salmon pink to blue natural sensitizers for solar cells: *Canna indica* L., *Salvia splendens*, cowberry and *Solanum nigrum* L., *Spectrochim. Acta, Part A*, 74 (4), 936–942.

[9] Narayan, M.R., 2012, Review: Dye-sensitized solar cells based on natural photosensitizers, *Renewable Sustainable Energy Rev.*, 16 (1), 208–215.

[10] Calogero, G., Yum, J.H., Sinopoli, A., Di Marco, G., Grätzel, M., and Nazeerudin, M.K., 2012,

Anthocyanins and betalains as light-harvesting pigments for dye-sensitized solar cells, *Solar Energy*, 86 (5), 1563–1575.

[11] Prabavathy, N., Shalini, S., Balasundaraprabhu, R., Velauthapillai, D., Prasanna, S., and Mutuhukumasamy, N., 2017, Enhancement in the photostability of natural dyes for dye-sensitized solar cells (DSSC) applications: a review, *Int. J. Energy Res.*, 41 (10), 1372–1396.

[12] Ma, J.G., Zhang, C.R., Gong, J.J., Wu, Y.Z., Kou, S.Z., Yang, H., Chen, Y.H., Liu, Z.J., and Chen, H.S., 2015, The electronic structures and optical properties of alkaline-earth metals doped anatase TiO_2: A comparative study of screened hybrid functional and generalized gradient approximation, *Materials*, 8 (8), 5508–5525.

[13] Nam, T.V., Trang, N.T., and Cong, B.T., 2012, Mg-doped TiO_2 for dye-sensitized solar cell: An electronic structure study, *Proc. Natl. Conf. Theor. Phys*, 37, 233–242.

[14] Ansari, S.G., Umar, A., Al-Hajry, A., Al-Deyab, S.S., and Ansari, Z.A., 2012, Effect of flower extracts on the optoelectronic properties of Cd and Sn dopes TiO_2 nanopowder, *Sci. Adv. Mater.*, 4, 763–770.

[15] Yildizhan, M.M., Sturm S., and Gulgun, M.A., 2016, Structural and electronic modification on TiO_2 anatase by Li, K or Nb doping below and above the solubility limit, *J. Mater. Sci.*, 51 (12), 5912–5923.

[16] Liu, Y., Zhou, W., Liang, Y., Cui, W., and Wu, P., 2015, Tailoring band structure of TiO_2 to enhance photoelectrochemical activity by codoping S and Mg, *J. Phys. Chem. C*, 119 (21), 11557–11562.

[17] Liu, Q.P., 2014, Photovoltaic performance improvement of dye-sensitized solar cells based on Mg-doped TiO_2 thin films, *Electrochim. Acta*, 129, 459–462.

[18] Frisch, M.J., Trucks, G.W., Schlegel, H.B., Scuseria, G.E., Robb, M.A., Cheeseman, J.R., Scalmani, G., Barone, V., Mennucci, B., Petersson, G.A., Nakatsuji, H., Caricato, M., Li, X., Hratchian, H.P., Izmaylov, A.F., Bloino, J., Zheng, G., Sonnenberg, J.L., Hada, M., Ehara, M., Toyota, K., Fukuda, R., Hasegawa, J., Ishida, M., Nakajima, T., Honda, Y., Kitao, O., Nakai, H., Vreven, T., Montgomery, Jr., J.A., Peralta, J.E., Ogliaro, F., Bearpark, M., Heyd, J.J., Brothers, E., Kudin, K.N., Staroverov, V.N., Kobayashi, R., Normand, J., Raghavachari, K., Rendell, A., Burant, J.C., Iyengar, S.S., Tomasi, J., Cossi, M., Rega, N., Millam, J.M., Klene, M., Knox, J.E., Cross, J.B., Bakken, V., Adamo, C., Jaramillo, J., Gomperts, R., Stratmann, R.E., Yazyev, O., Austin, A.J., Cammi, R., Pomelli, C., Ochterski, J.W., Martin, R.L., Morokuma, K., Zakrzewski, V.G., Voth, G.A., Salvador, P., Dannenberg, J.J., Dapprich, S., Daniels, A.D., Farkas, Ö., Foresman, J.B., Ortiz, J.V., Cioslowski, J., and Fox, D.J., 2009, *Gaussian 09, Revision D.01*, Gaussian, Inc., Wallingford.

[19] McLean, A.D., and Chandler, G.S., 1980, Contracted Gaussian basis sets for molecular calculations. I. Second-row atoms, Z=11–18, *J. Chem. Phys.*, 72 (10), 5639–5648.

[20] Hanwell, M.D., Curtis, D.E., Lonie, D.C., Vandermeersch, T., Zurek, E., and Hutchison, G.R., 2012, Avogadro: An advanced semantic chemical editor, visualization, and analysis platform, *J. Cheminform.*, 4, 17.

[21] Gao, L., Li, Y., Ren, J., Wang, S., Wang, R., Fu, G., and Hu, Y., 2017, Passivation of defect states in anatase TiO_2 hollow spheres with Mg doping: Realizing efficient photocatalytic overall water splitting, *Appl. Catal., B*, 202, 127-133.

[22] Kumar, M., Gupta, A.K., and Kumar, D., 2016, Mg-doped TiO_2 thin films deposited by low-cost technique for CO gas monitoring, *Ceram. Int.*, 42 (1), 405–410.

[23] Liu, Z., Jian, Z., Fang, J., Xu, X., and Wu, S., 2012, Low-temperature reverse microemulsion synthesis, characterization, and photocatalytic performance of nanocrystalline titanium dioxide, *Int. J. Photoenergy*, 2012, 702503.

[24] Mali, S.S., Shinde, P.S., Betty, C.A., Bhosale, P.N., Lee, W.J., and Patil, P.S., 2011, Nanocoral architecture of TiO_2 by hydrothermal process: Synthesis and characterization, *Appl. Surf. Sci.*, 257 (23), 9737–9746.

[25] Sengupta, D., Mondal, B., and Mukherjee, K., 2015, Visible light absorption and photo-sensitizing properties of spinach leaves and beetroot extracted natural dyes, *Spectrochim. Acta, Part A*, 148, 85–92.

[26] Chen, Y., Zhao, S., Chen, M., Zhang, W., Mao, J., Zhao, Y., Maitz, M.F., Huang, N., and Wang, G., 2015, Sandwiched polydopamine (PDA) layer for titanium dioxide (TiO_2) coating on magnesium to enhance corrosion protection, *Corros. Sci.*, 96, 67–73.